KFUPM
Journal of Undergraduate Research International

Diamond Open Access 127

Article Material Science and Engineering

Influence of Halogen Incorporation on the Structural and Electrocatalytic Properties of Co-Based Metal-Organic Frameworks

Alanood Alduraibi and Abuzar Khan*

Cite https://doi.org/10.64589/juri/231622

Submitted: April 25, 2026 **Revised:** June 06, 2026 **Accepted:** July 09, 2026

ABSTRACT

Developing efficient electrocatalysts is essential for producing green hydrogen via water splitting. In this study, halogen-doped cobalt benzene-1,4-dicarboxylate (Co-BDC) metal-organic frameworks (MOFs) were synthesized by incorporating F, Br, and I. Structural characterization through X-ray diffraction, Fourier-transform infrared spectroscopy, and transmission electron microscopy confirmed that the halogens were successfully incorporated while preserving the crystalline framework. Electrochemical measurements showed that incorporating the halogenss (F, Br and I) significantly enhanced the catalytic performance compared with that of the pristine Co-BDC. Notably, the Br-doped Co-MOF exhibited the highest water-splitting activity, with a lower overpotential and improved charge-transfer kinetics. This improvement is attributed to the structural and surface modifications of the Co centers, which facilitate the reaction intermediate adsorption. These findings demonstrate that halogen functionalization is an effective strategy for engineering high-performance MOF-based electrocatalysts.

Keywords: Halogen doping; Cobalt-benzene-1,4-dicarboxylate metal-organic framework; Alkaline water splitting; Synergistic halogen effects

1. INTRODUCTION

Producing green hydrogen via water electrolysis enables sustainable low-carbon energy generation, with alkaline and acidic media commonly used for electrolysis[1]. Although acidic electrolysis achieves high efficiency, it causes severe corrosion, and requires highly stable and expensive materials[2,3]. Alkaline electrolysis is more cost-effective and utilizes abundant catalytic materials[4,5]. Noble metals are effective electrocatalysts for the hydrogen evolution reaction (HER), given their high stability and low overpotential[6]. However, their scarcity and high cost limit their application, motivating the development of earth-abundant alternatives. Transition-metal-based catalysts are more abundant and exhibit favorable catalytic activity[7]. Among these, Co offers suitable electronic properties, chemical stability, and compatibility with alkaline media. Nevertheless, pristine Co-based catalysts suffer from relatively high overpotentials and limited HER efficiencies, which stem from the electronic properties of Co and its interactions with intermediate species, affecting the adsorption-desorption behavior. Recently, metal-organic frameworks (MOFs) have emerged as nanostructured electrocatalysis materials, particularly from energy storage and conversion[8]. MOFs consist of metal centers coordinated with organic linkers, and offer a high surface area, tunable porosity, and flexible structural geometry, which render them attractive catalysts for both acidic and alkaline systems. Specifically, Co-based MOFs offer abundant active sites and structural flexibility[9].

However, their low conductivities and limited electron-transfer capabilities restrict their electrochemical performance. Several strategies, including thermal treatment and structural engineering, have been explored to overcome these limitations. Although high-temperature treatment can improve the conductivity, it may alter the MOF framework and introduce synthesis complexities[10]. Therefore, developing modification strategies that enhance the electrochemical properties of MOFs while preserving their MOF structures is important. Incorporating suitable dopants[11] into the MOF can tune the local electronic environment, increase the number of active sites, and optimize the adsorption-desorption kinetics of the reaction intermediates. Halogens such as F, Br, and I are attractive dopants, as they can influence the charge distribution within the material, and induce structural and electronic modifications that enhance the charge-transfer and catalytic activity[12].

In this study, pristine and halogen-modified Co-MOF catalysts were synthesized using a solvothermal method[13,14] to evaluate the impact of different halogen modifications on the structural, chemical, and morphological properties and the HER performance. Thus, this study clarifies the role of halogen incorporation in improving the structural and electrocatalytic properties of Co-MOF catalysts.

2. MATERIALS AND METHODS

2.1. Preparation of Co-MOFs and Halogen-Modified Variants. The Co-MOF was synthesized using Co nitrate hexahydrate ($Co(NO_3)_2 \cdot 6H_2O$) as the Co source and

Published under an exclusive license by KFUPM

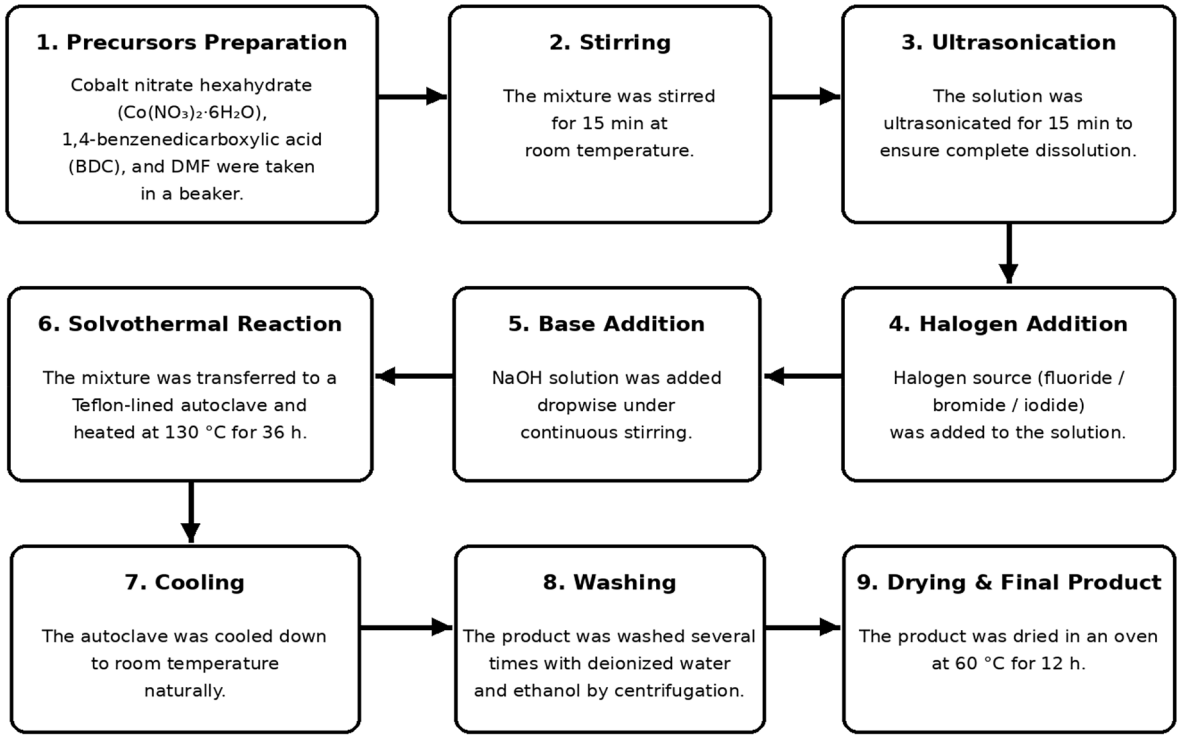


Figure 1. Synthesis of pristine and halogen-modified Co-metal-organic framework (MOFs) via a solvothermal method

1,4-benzenedicarboxylic acid (BDC, 402 mg) as the organic linker using 15 mL of N,N-dimethylformamide (DMF) as the solvent. The mixture was stirred to ensure complete dissolution, after which 2.5 mL of 2 M NaOH solution was introduced gradually under continuous stirring. The resulting solution was ultrasonicated for 15 min to produce a homogeneous mixture. Then, this reaction solution was transferred into a Teflon-lined autoclave, and maintained at 130 °C for 36 h under solvothermal conditions. The resulting solid, designated as the Co-MOF, was separated after the solvothermal reaction, washed using ethanol and deionized water before being oven-dried at 60 °C for 12 h, for subsequent use.

For synthesizing the halogen-modified samples, the halogen source was added at a fixed 1:1 molar ratio relative to the Co precursor to ensure a consistent modification across all samples. In all the cases, BDC (402 mg) was used as the organic linker. The Co salt and selected halogen sources (i.e., F, Br, and I) were first dissolved using 15 mL of DMF and mixed for 15 min until completely dissolved. Subsequently, 2 M NaOH (2.5 mL) was added while stirring, after which the mixture underwent sonication for 15 min prior to solvothermal treatment. Then, this mixture was placed in a Teflon-lined autoclave and maintained at 130 °C for 36 h. Once cooled, the products were recovered through centrifugation, rinsed with ethanol and deionized water, before being oven-dried at 60 °C for 12 h. The obtained materials were designated Co-MOF/F, Co-MOF/Br, and Co-MOF/I, according to the incorporated halogen elements [13,14].

2.2. Preparation of the MOF-Modified Electrodes. The synthesized MOFs were deposited onto nickel foam (NF) through a drop-casting procedure. The MOF powders were suspended in methanol to produce a uniform suspension before application, to achieve an even coating. Each NF substrate was loaded with approximately 1 mg cm^{-2} of the catalyst. After depositing the catalyst layer, the electrode was coated with 15 μL of a 5% Nafion solution in ethanol and then dried under vacuum for 30 min. In the electrochemical evaluation, the halogen-modified Co-MOFs showed a superior electrocatalytic performance compared with the pristine Co-MOF, confirming the beneficial effect of halogen incorporation. Therefore, the optimized samples were selected for further physicochemical and electrochemical characterization [15–17].

2.3. Material Characterization. Several characterization methods were used to evaluate the structural, chemical, and morphological features of the as-synthesized Co-MOF samples. Fourier transform infrared (FTIR) spectroscopy was utilized to determine the functional groups and bonding characteristics. Powder X-ray diffraction (XRD) was used to evaluate the crystal structure and phase composition. Surface morphology was examined using scanning electron microscopy (SEM), and transmission electron microscopy (TEM) was employed to examine the morphology and internal structure of the materials. Energy-dispersive X-ray spectroscopy (EDS), combined with elemental mapping, was performed to verify the elemental composition and spatial distribution of the halogen dopants.

The electrochemical performance for the HER was evaluated with a three-electrode configuration under an alkaline medium. The catalyst supported on NF served as the working electrode, whereas Hg/HgO and a platinum electrode functioned as the reference and counter electrodes, respectively. A 1.0 M KOH solution served as the electrolyte. Linear sweep voltammetry (LSV) was performed to evaluate the HER activity [7,8,17]. Electrochemical impedance spectroscopy (EIS) was employed to examine the charge-transfer resistance and interfacial behavior. The Nyquist plots were fitted with a simple equivalent circuit

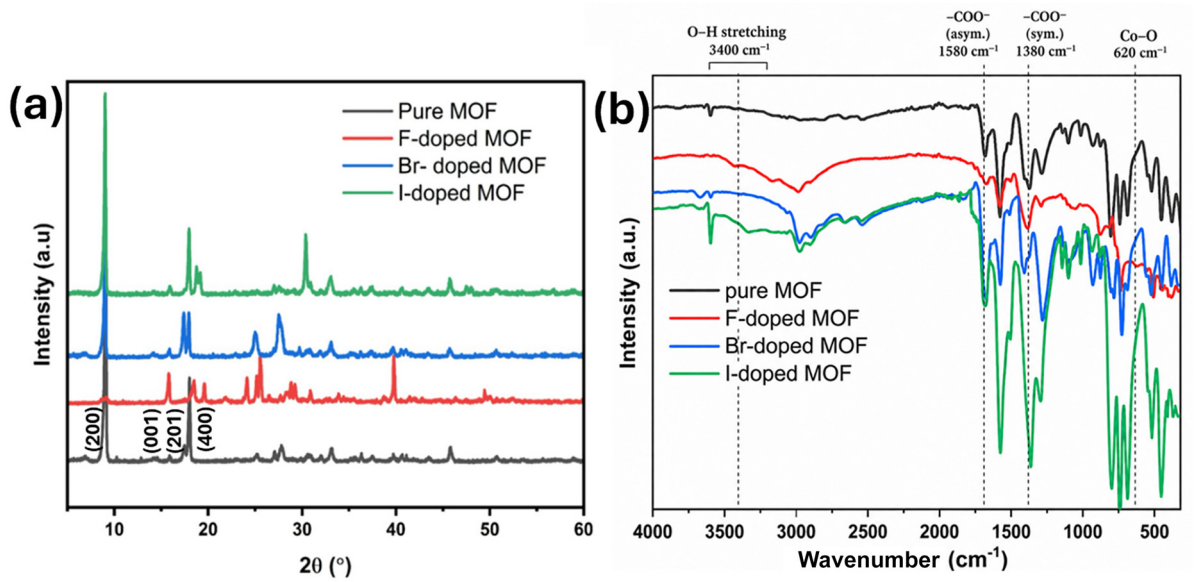


Figure 2. Comparative (a) X-ray diffraction (XRD) patterns and (b) Fourier-transform infrared (FTIR) spectra of pure, F-doped, Br-doped, and I-doped MOFs, confirming their high crystallinity and the successful coordination between the Co centers and benzene-1,4-dicarboxylate (BDC) linkers in all the samples

comprising a solution resistance (R_s) connected in series with a parallel arrangement of the charge transfer resistance (R_{ct}) and double layer capacitance (C_{dl})[18]. The long-term stability was assessed by chronoamperometry under a current density of 10 mA cm^{-2} [19].

3. RESULTS AND DISCUSSION

3.1. Physicochemical Analysis.

3.1.1. Structural and chemical analysis. The crystal structures of the pristine and halogen-modified Co-MOFs were analyzed using powder XRD. As shown in Fig. 2(a), all the samples exhibit distinct diffraction peaks, confirming their crystalline nature. The pristine Co-MOF shows well-defined diffraction peaks consistent with previously reported Co-BDC framework structures, with characteristic peaks at approximately $2\theta = 9.7°$, 17.5°, 26.3°, 31.2°, and 41.8°. After halogen incorporation, only slight changes in the peak intensity and minor peak shifts were observed, indicating lattice distortion without destroying the main Co-MOF. The absence of additional impurity peaks confirms the phase purity of the synthesized samples. The crystal structure of the pristine Co-MOF aligned well with the data from the Cambridge Crystallographic Data Centre (No. 153067).

FTIR spectroscopy was used to examine the functional groups present in the MOFs. The FTIR spectra of Co-MOF, Co-MOF/F, Co-MOF/Br, and Co-MOF/I are presented in Fig. 2(b). All the samples exhibit similar characteristic bands, indicating a successful coordination between the Co centers and BDC ligands. The bands at approximately 1580 and 1380 cm^{-1} are assigned to the asymmetric and symmetric stretching modes of the carboxylate ($–COO^-$) groups, respectively. The low-wavenumber band at approximately 620 cm^{-1} corresponds to the Co-O vibrations in the MOF, while the broad band at approximately 3400 cm^{-1} is attributed to the O-H stretching of the adsorbed or coordinated water molecules. These vibrational features agree with those of reported Co-MOF structures and confirm the formation of the BDC-based framework. The structural and chemical characteristics are further supported by the morphological analysis discussed in Section 3.1.2 [13,14,20].

SEM was used to investigate the surface morphology of the synthesized samples (Fig. 3). The pristine Co-MOF (Fig. 3(a)) exhibited a rod-like crystalline morphology with distinct faceted structures, indicating a well-defined crystal growth. Clear morphological changes were observed after the halogen incorporation. The F-doped Co-MOF (Fig. 3(b)) showed densely packed granular aggregates, whereas the Br-doped sample (Fig. 3(c)) showed elongated needle-like structures with an increased surface roughness. The I-doped Co-MOF (Fig. 3(d)) exhibited an interconnected sheet-like morphology, forming a more open porous network. These variations suggest that the halogen incorporation influences the crystal growth kinetics and self-assembly behavior, which may contribute to the observed differences in the electrochemical performance [12,14,21].

3.1.2. Morphological analysis. EDS analysis was performed to confirm the elemental compositions of the pristine and halogen-modified Co-MOF samples. The pristine Co-MOF contained C, O, and Co at 45.1, 30.8, and 24.0 wt.%, respectively (Fig. 4(a-d)). After the halogen incorporation, the corresponding halogen signals were detected in the modified samples, i.e., F in Co-MOF/F (10.8 wt.%), Br in Co-MOF/Br (0.1 wt.%), and I in Co-MOF/I (0.2 wt.%). These results confirm the successful incorporation of the halogen species into the Co-MOF structure while preserving the C-O-Co framework composition.

Figure 5 shows the elemental mapping used to examine the spatial distribution of the main elements in the pristine and halogen-modified Co-MOF samples. The maps show that Co, O, and C are distributed throughout the selected regions in all the samples, confirming the preservation of the Co-MOF. In the modified samples, the corresponding halogen elements

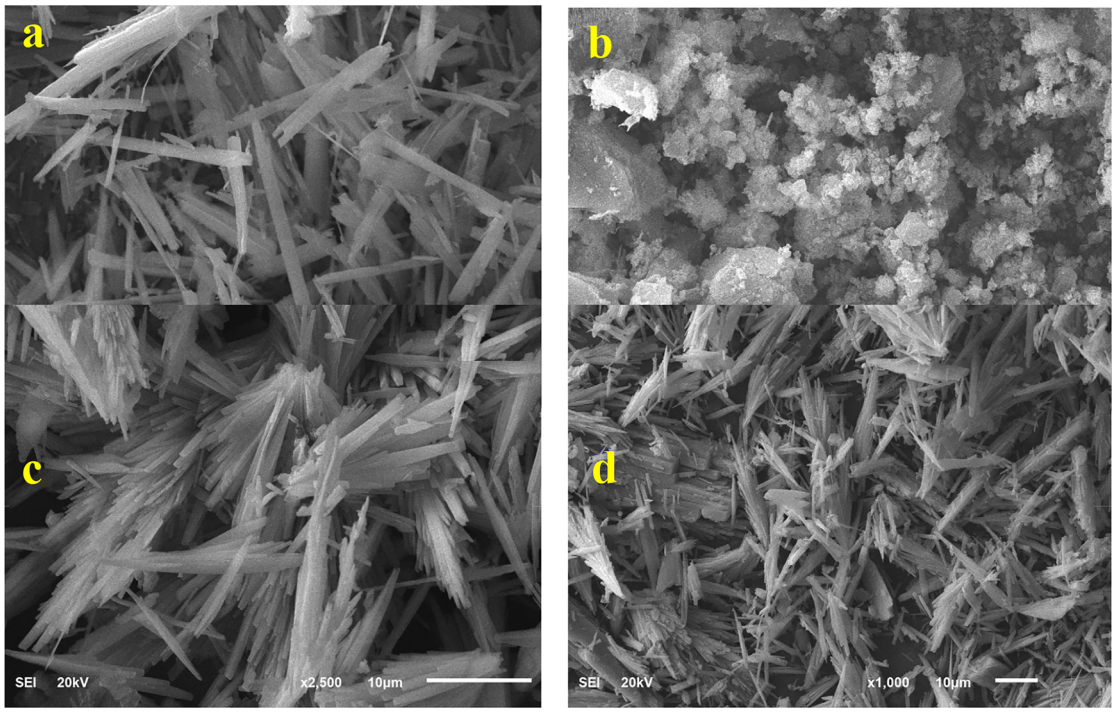


Figure 3. Scanning electron microscopy (SEM) images of (a) pristine Co-MOF, (b) F-doped Co-MOF, (c) Br-doped Co-MOF, and (d) I-doped Co-MOF, showing the morphological changes induced by the halogen incorporation

(F, Br, and I) are also seen within the mapped areas, confirming the successful incorporation of the different halogens. The absence of obvious element-rich regions suggests that the halogens were incorporated without forming large, separate impurity domains.

Transmission electron microscopy (TEM), high-resolution TEM (HRTEM), and selected area electron diffraction (SAED) analyses were conducted to examine the morphology, nanoscale structure, and crystallinity of the prepared samples. As shown in Fig. 6, the pristine and halogen-modified Co-MOF catalysts display noticeable morphological differences. The pristine Co-MOF exhibits a flake-like morphology with well-dispersed nanoscale features. By contrast, the halogen-modified samples show increased aggregation and sheet-like structures, forming

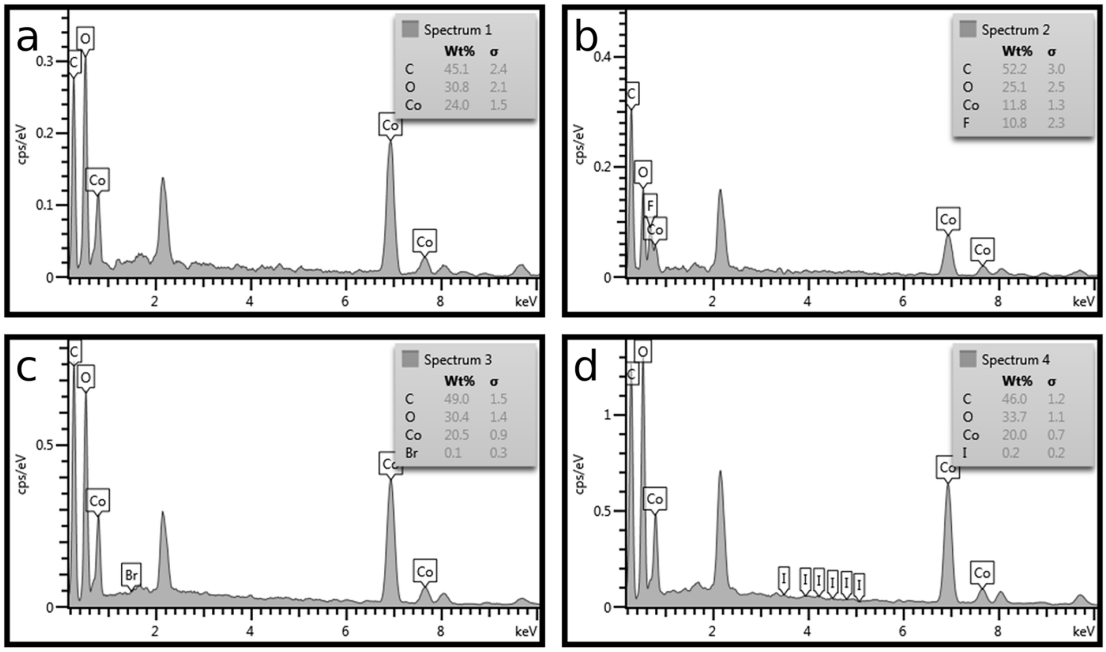


Figure 4. Energy-dispersive X-ray spectroscopy (EDS) spectra of (a) pristine Co-MOF, (b) Co-MOF/F, (c) Co-MOF/Br, and (d) Co-MOF/I, showing the elemental compositions of the samples and confirming the detection of the corresponding halogen elements (F, Br, and I) after modifications

flower-like morphologies. These changes are consistent with the lattice distortion induced by incorporating the halogens. The modified samples, i.e., Co-MOF/F, Co-MOF/Br, and Co-MOF/I, similarly exhibit aggregated sheet-like features, suggesting that the halogen incorporation promotes the MOF sheet assembly through a charge imbalance and local structural distortion [12,21]. No distinct impurity phases or isolated metal particles were observed, confirming the successful formation and purity of the synthesized Co-MOFs. The SAED patterns further confirm the crystalline nature of the samples. Overall, the TEM results demonstrate that halogen incorporation modifies the morphology of the Co-MOF framework while maintaining its structural integrity.

3.2. Electrochemical Evaluation. The electrocatalytic performance of the synthesized MOF-based catalysts with the different halogen modifications was evaluated in 1.0 M KOH to assess their catalytic efficiency (Fig. 7). The LSV curves of the different electrodes are shown in Fig. 7(a). Incorporating the halogens into the Co-MOF improved the HER activity significantly. Among the tested materials, the Br-doped MOF exhibited the best performance, requiring an overpotential of 250 mV to reach 10 mA cm^{-2}, compared with 275, 280, and 312 mV for the I-doped, F-doped, and pristine MOFs, respectively.

The overpotentials at 10 mA cm^{-2} are summarized in Fig. 7(b) to compare the catalytic activity at a fixed current density. The Br-doped MOF shows the lowest overpotential, followed by the I- and F-doped samples, whereas the pristine MOF requires the highest overpotential. This trend confirms that the halogen incorporation, particularly the Br-doping, effectively reduces the kinetic barrier for the HER. The corresponding Tafel slopes (Fig. 7(c)) provide further insights into the HER kinetics. The Br-doped MOF exhibits the smallest Tafel slope of 86 mV dec^{-1}, compared with slopes of 98, 107, and 125 mV dec^{-1} for the I-doped, F-doped, and pristine MOFs, respectively. The lower Tafel slope of Co-MOF/Br indicates more favorable reaction kinetics, which is consistent with its lowest overpotential.

These catalytic activity trends can be rationalized by considering the basic periodic properties of the halogen dopants. F has the highest electronegativity and smallest ionic radius, which can result in strong electron withdrawal from the Co centers and somewhat limit the HER rate, whereas I has the lowest electronegativity and largest ionic radius, which can cause a stronger lattice distortion and a less optimal local environment. Br lies between F and I in terms of both the electronegativity and size, and provides a more balanced adjustment of the Co sites and framework, which is consistent with the lowest overpotential and charge-transfer resistance observed for the Br-doped sample in this study [12]. Therefore, the superior performance of the Br-doped MOF may be attributed to its intermediate electronegativity (2.96), which offers a balance between the local electronic effects and structural stability. By contrast, F (electronegativity = 3.98) may cause an excessive electron withdrawal, whereas I (electronegativity = 2.66) may provide insufficient modulation and introduce a structural disruption owing to its larger ionic radius. These results suggest that the halogen incorporation reduces the overpotential by altering the Co environment and improving the charge-transfer behavior.

However, the excessive structural distortion caused by the larger halogen atoms may somewhat limit the catalytic performance. Therefore, the observed improvements in the HER activity can be associated with a balanced halogen incorporation and the resulting structural changes, although the electrochemically active surface area was not measured in this study. In addition to the overpotential and Tafel analyses, EIS was performed to investigate the charge-transfer kinetics [18]. In this circuit, the Rct value indicates the charge transfer kinetics at the electrode–electrolyte

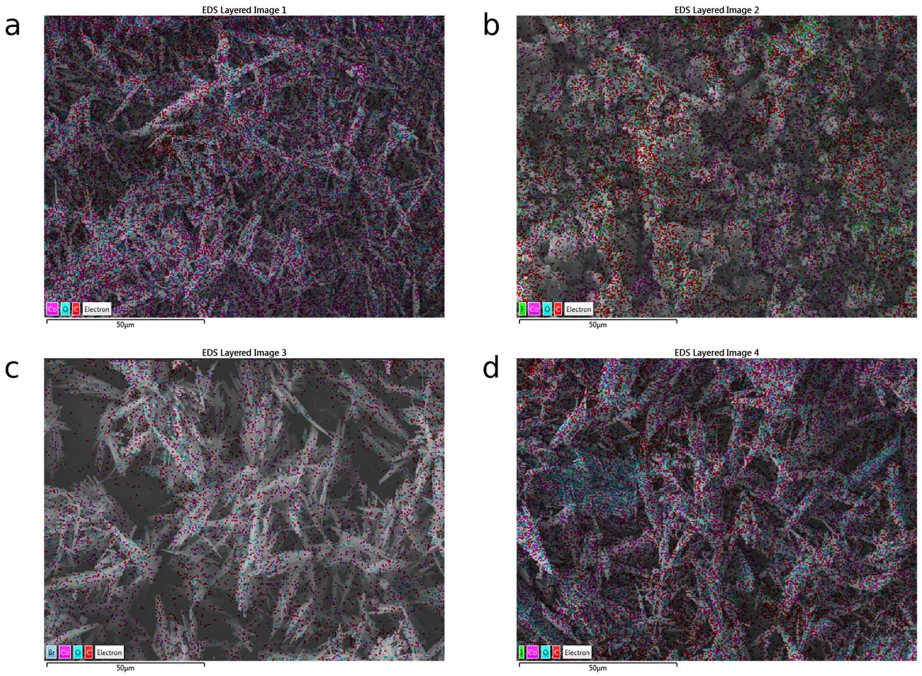


Figure 5. EDS elemental mapping images of (a) pristine Co-MOF, (b) Co-MOF/F, (c) Co-MOF/Br, and (d) Co-MOF/I, showing the spatial distribution of Co, O, C, and the corresponding halogen elements within the mapped regions

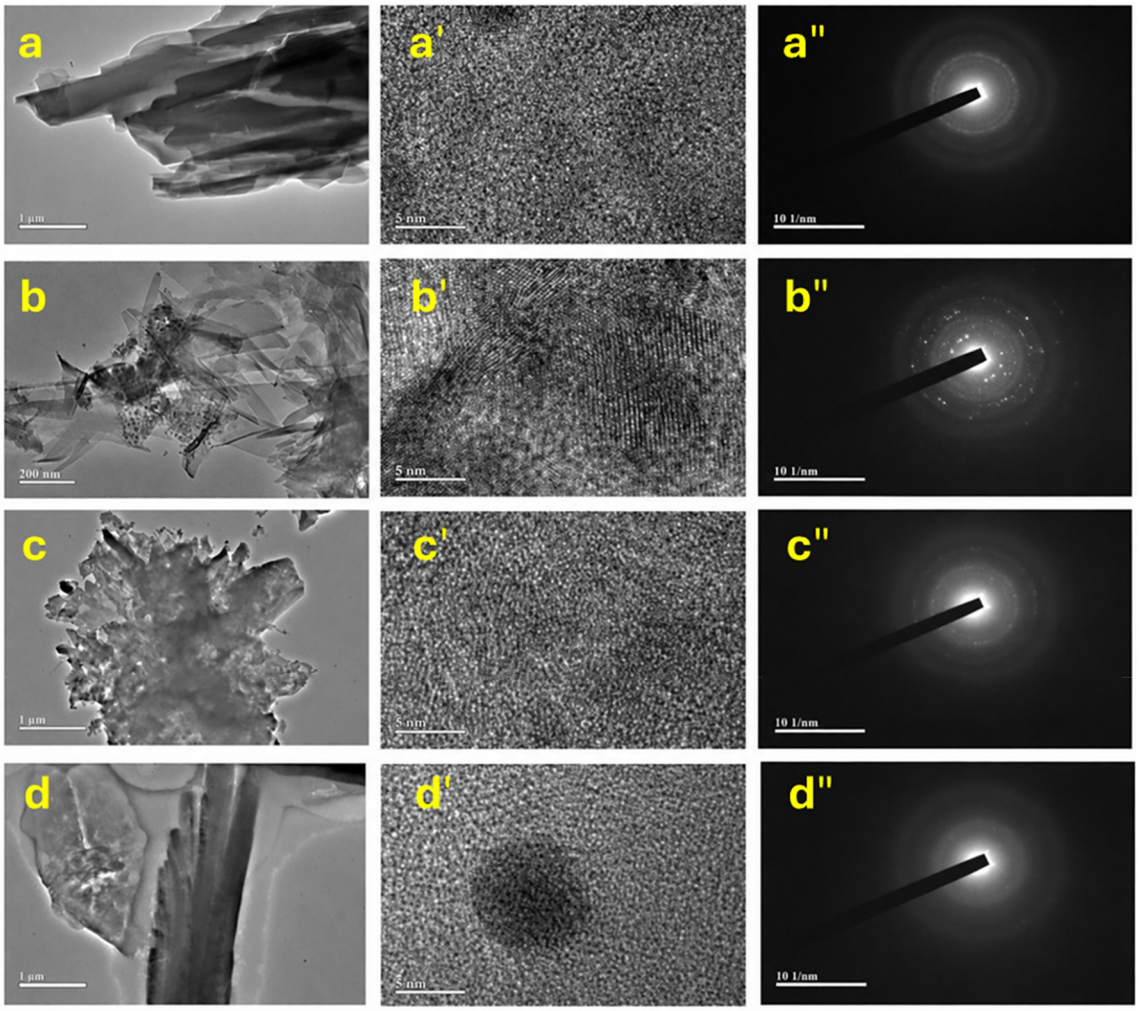


Figure 6. Transmission electron microscopy (TEM), high-resolution TEM (HRTEM), and selected area electron diffraction (SAED) images of the pristine and halogen-modified Co-MOF samples: (a) Co-MOF shows a flake-like morphology with uniformly dispersed nanoscale features, (b) Co-MOF/F, (c) Co-MOF/Br, and (d) Co-MOF/I exhibit agglomerated sheet-like structures forming flower-like morphologies. SAED patterns confirm the crystalline nature of all the samples

interface. As shown in Fig. 7(d), the Nyquist plots reveal that the halogen-doped MOFs had smaller semicircle diameters than that of the pristine Co-MOF, indicating a lower charge-transfer resistance and improved electron-transfer kinetics. The Br-doped MOF exhibited the lowest resistance, confirming its superior catalytic activity.

Further, the electrochemical stability of the optimized Br-doped MOF catalyst was evaluated by chronoamperometry at 10 mA cm^{-2} (Fig. 7(e)). The current density exhibited a good retention over the testing period, indicating stable catalytic behavior under alkaline conditions [19]. Overall, the electrochemical results indicate that the halogen doping enhances the catalytic performance of the MOF-based electrodes by improving the charge-transfer, reducing the overpotential, and increasing the stability, thus making them promising candidates for HER applications.

The HER performance of Co-MOF/Br was compared with selected Co-based and MOF-derived electrocatalysts reported in the literature, under alkaline conditions, to evaluate the electrocatalytic relevance of the optimized catalyst. Co-MOF/Br showed improved catalytic behavior compared with the pristine Co-MOF, as indicated by its lower overpotential, reduced charge-transfer resistance, smaller Tafel slope, and stable chronoamperometric response at 10 mA cm^{-2} in 1.0 M KOH. The comparison places the Br-doped MOF within a competitive range relative to the reported Co-MOF and Co-MOF-derived HER electrocatalysts, supporting the effectiveness of halogen incorporation as a simple and scalable strategy for enhancing MOF-based HER catalysts [16,17,22].

4. CONCLUSIONS

In this study, halogen-modified Co-BDC MOFs were successfully prepared using a solvothermal approach to enhance their electrocatalytic performance in terms of alkaline water splitting. Comprehensive physicochemical characterization was performed using XRD, FTIR, SEM, TEM, EDS, and elemental mapping to confirm the crystallinity, phase purity, elemental composition, and morphology of the MOFs. Incorporating the halogens (F, Br, and I) induced beneficial lattice distortions and structural aggregation into flower-like morphologies. The electrochemical results suggest that halogen doping modifies the local environment of the Co sites and is associated with improved

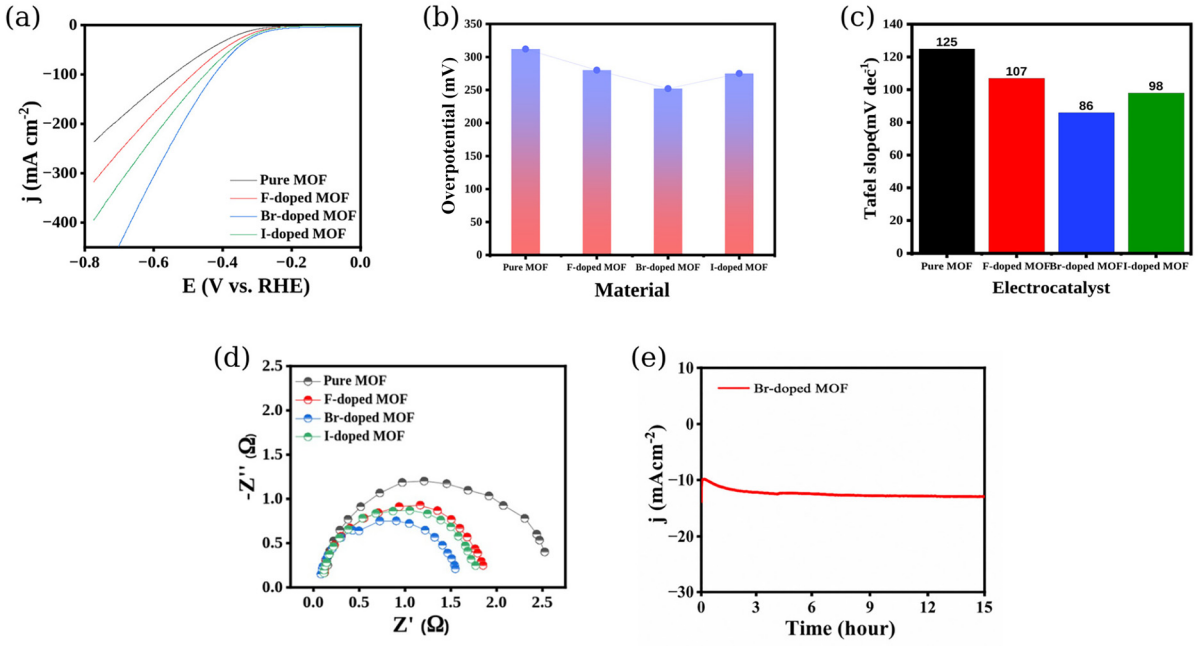


Figure 7. Electrochemical performance in 1.0 M KOH: (a) Linear sweep voltammetry (LSV) curves of the pristine and halogen-doped MOF electrodes, (b) overpotential at 10 mA cm^{-2}, (c) Tafel slopes, (d) electrochemical impedance spectroscopy (EIS) Nyquist plots showing the charge-transfer resistance, and (e) chronoamperometry stability test at 10 mA cm^{-2}

charge-transfer kinetics. Among the catalysts investigated, Co-MOF/Br exhibited the best activity, characterized by the lowest overpotential and smallest charge-transfer resistance. The optimized catalyst also exhibited good long-term stability in 1.0 M KOH. These findings affirm that halogen functionalization is an effective strategy for modulating the intrinsic properties of transition-metal-based MOFs in clean-energy applications.

Future studies should focus on optimizing the halogen incorporation conditions and further investigating the relationship between structural modifications and electrocatalytic performance. In addition, evaluating these catalysts under extended operating conditions could provide further insight into their potential for practical water-electrolysis applications.

AFFILIATIONS AND AUTHOR DETAILS

Undergraduate Author

Alanood Alduraibi – *Department of Materials Science & Engineering, King Fahd University of Petroleum & Minerals, Dhahran 31261, Saudi Arabia;* 0009-0008-4812-6450
Email: s202350370@kfupm.edu.sa

Corresponding Author

Abuzar Khan – *Research Mentor, Professor, Interdisciplinary Center for Hydrogen Technologies and Carbon Management, King Fahd University of Petroleum & Minerals, Dhahran 31261, Saudi Arabia;* 0000-0001-9122-2247
Email: abuzar@kfupm.edu.sa

REFERENCES

(1) Raveendran, A., Chandran, M. & Dhanusuraman, R. A comprehensive review on the electrochemical parameters and recent material development of electrochemical water splitting electrocatalysts. *RSC Advances* 13, 3843–3876 (2023).

(2) Meng, Q., *et al.* Corrosion behavior of metallic coatings on titanium bipolar plates of proton exchange membrane water electrolysis. *Int. J. Hydrogen Energy* **63**, 1105–1115 (2024).

(3) Qadir, A. *et al.* Advancements in acidic OER and HER electrocatalysts: iridium, MOF-based, and ruthenium systems for sustainable hydrogen production. *Int. J. Hydrogen Energy* **152**, 150188 (2025).

(4) Dilpazir, S. *et al.* A biomass-derived jute carbon integrated FeCoNi alloy as a robust catalyst for alkaline water splitting. *J. Mater. Chem. A* **13**, 25892–25903 (2025).

(5) Dastafkan, K. & Zhao, C. Recent trends in alkaline hydrogen evolution using nonprecious multi-metallic electrocatalysts. *Curr. Opin. Green Sustain. Chem.* **25**, 100342 (2020).

(6) Li, C. & Baek, J.-B. Recent advances in noble metal (Pt, Ru, and Ir)-based electrocatalysts for efficient hydrogen evolution reaction. *ACS Omega* **5**, 31–40 (2020).

(7) Sun, R. *et al.* Recent advances in cobalt-based catalysts for efficient electrochemical hydrogen evolution: a review. *Dalton Trans.* **51**, 15205–15226 (2022).

(8) Ali, M. *et al.* Recent advancements in MOF-based catalysts for applications in electrochemical and photoelectrochemical water splitting: a review. *Int. J. Energy Res.* **45**, 1190–1226 (2021).

(9) Zhang, J. *et al.* Research progress of cobalt-based metal-organic frameworks and their derivatives in energy storage and conversion. *ACS Omega* **9**, 46643–46663 (2024).

(10) Sun, L., Campbell, M. G. & Dincă, M. Electrically conductive porous metal-organic frameworks. *Angew. Chem. Int. Ed.* **55**, 3566–3579 (2016).

(11) Wang, J. *et al.* Heteroatom-doping of non-noble metal-based catalysts for electrocatalytic hydrogen evolution: an electronic structure tuning strategy. *Small Methods* **5**, 2000988 (2021).

(12) Wu, L. *et al.* Halogen-assisted Ni-based MOFs ball-flowers for enhanced electrocatalytic oxygen evolution. *Int. J. Hydrogen Energy* **58**, 1295–1301 (2024).

(13) Snowlin, V. *et al.* Facile solvothermal fabrication of cobalt-metal-organic framework (Co-MOF)-based electrode material for supercapacitor devices. *J. Mater. Sci. Mater. Electron.* **36**, 1512 (2025).

(14) Bhoite, A. A., Sawant, V. A. & Tarwal, N. L. Solvothermal synthesis of Ni/Co-based metal-organic framework with nanosheets-like structure for high-performance supercapacitor. *Colloids Surf. A* **702**, 134814 (2024).

(15) Duan, J., Chen, S. & Zhao, C. Ultrathin metal-organic framework array for efficient electrocatalytic water splitting. *Nat. Commun.* **8**, 15341 (2017).

(16) Dong, J., Lv, C., Humphrey, M. G., Zhang, C. & Huang, Z. One-dimensional amorphous cobalt(II) metal-organic framework nanowire for efficient hydrogen evolution reaction. *Inorg. Chem. Front.* **9**, 4184–4193 (2022).

(17) Han, W., Li, M., Ma, Y. & Yang, J. Cobalt-based metal-organic frameworks and their derivatives for hydrogen evolution reaction. *Front. Chem.* **8**, 592915 (2020).

(18) Barsoukov, E. & Macdonald, J. R. *Impedance Spectroscopy: Theory, Experiment, and Applications* 2nd edn (Wiley-Interscience, 2005).

(19) Zhang, Y., Gao, L., Hensen, E. J. M. & Hofmann, J. P. Evaluating the stability of Co2P electrocatalysts in the hydrogen evolution reaction for both acidic and alkaline electrolytes. *ACS Energy Lett.* **3**, 1360–1365 (2018).

(20) Hua, Y., Li, X., Chen, C. & Pang, H. Cobalt-based metal-organic frameworks and their derivatives for electrochemical energy conversion and storage. *Chem. Eng. J.* **370**, 37–59 (2019).

(21) Łuczak, J., *et al.* Morphology control through the synthesis of metal-organic frameworks. *Adv. Colloid Interface Sci.* **314**, 102864 (2023).

(22) Łukasik, N., *et al.* Hydrogen evolution reaction catalyzed by Co-based metal-organic frameworks and their derivatives. *Int. J. Hydrogen Energy* **92**, 90–101 (2024).